



Cite this: *Phys. Chem. Chem. Phys.*, 2021, **23**, 20560

Unraveling the structural transition mechanism of room-temperature compressed graphite carbon†

Sheng-cai Zhu *^a and Qing-yang Hu ^{b,c}

HPSTAR
1228-2021

The discovery of graphite transition to transparent and superhard carbons under room-temperature compression (Takehiko, *et al.*, *Science*, 1991, **252**, 1542 and Mao, *et al.*, *Science*, 2003, **302**, 425) launched decades of intensive research into carbon's structural polymorphism and relative phase transition mechanisms. Although many possible carbon allotropes have been proposed, experimental observations and their transition mechanisms are far from conclusive. Three longstanding issues are: (i) the speculative structures inferred by amorphous-like XRD peaks, (ii) sp^2 and sp^3 bonding mixing, and (iii) the controversies of transition reversibility. Here, by utilizing the stochastic surface walking method for unbiased pathway sampling, we resolve the possible atomic structure and the lowest energy pathways between multiple carbon allotropes under high pressure. We found that a new transition pathway, through which graphite transits to a highly disordered phase by shearing the boat architecture line atoms out of the graphite (001) plane upward or downward featuring without the nuclei core, is the most favorable. This transition pathway facilitates the generation of a variety of equally favorable carbon structures that are controlled by the local strain and crystal orientation, resembling structural disordering. Our results may help to understand the nature of graphite under room temperature compression.

Received 26th July 2021,
Accepted 26th August 2021

DOI: 10.1039/d1cp03415d

rsc.li/pccp

The solid–solid phase transition is widely known to be sensitive to a number of factors, such as local stress, pressure and temperature. The physical properties of the materials are determined by their micro-structures, which are usually pathway-dependent. Graphite is the ground state of carbon at ambient conditions.^{1,2} The (001) basal plane of graphite spreads extensively due to the delocalized π -electrons on the honeycomb carbon sheets. The chair line and boat line are the two signature architecture lines on the basal plane. As shown in Fig. 1a, because the thickness of the (001)_{GR} plane is much greater than that of the (100)_{GR} plane, graphite is known to exhibit strong anisotropic behaviors.³ It has been well documented that under room temperature compression, graphite can undergo solid–solid phase transition to an unrecoverable superhard material. In contrast, it transforms into a hexagonal diamond (HD, *P63/mmc*, #194) and/or cubic diamond (CD, *Fd3m*, #227) at high-temperature and high-pressure.^{4–7}

However, the room-temperature compressed phases often have blurry XRD patterns,⁸ and were reported to be unrecoverable to ambient pressure.⁹ This makes their atomic structure still unclear, nor to say the transition kinetics.

Understanding the nature of carbon polymorphism under room-temperature compression has attracted much research interest.¹⁰ By measuring the electrical resistance, Aust and Drickamer⁴ found a sudden increase of resistance once single crystal graphite is pressurized to 15 GPa, and the resistance continues to rise with pressure. Montgomery *et al.*¹¹ found that the resistance of graphite evolves as a function of time, indicating that the phase transition kinetics is sluggish. For the high-pressure structure, Bundy⁹ regarded it as the HD, but also realized that this phase is unquenchable unless the temperature keeps as high as 1000 °C. Yagi *et al.*¹² agreed that the high-pressure carbon is HD. However, they later suggested that the high-pressure phase occupies a different structure from HD,¹³ and it is unquenchable without heating. Their claims were supported by Hanfland *et al.*,^{7,14} who found that the high pressure phase reverses to graphite when it was depressurized to below 2 GPa at room temperature. With decompression under constrained kinetics, *e.g.*, between 15 and 30 K, Miller *et al.*⁵ found this high pressure carbon can be recovered to ambient pressure. However, the sample color darkens between 130 and 170 K, and eventually became opaque at 260 K. Squeezing in a pair of sapphire anvil cells to avoid the noisy

^a School of Materials, Sun Yat-sen University, Guangzhou 510275, China.

E-mail: zhushc@mail.sysu.edu.cn

^b Center for High Pressure Science and Technology Advanced Research (HPSTAR), Beijing 100094, P. R. China

^c CAS Center for Excellence in Deep Earth Science, Guangzhou Institute of Geochemistry, Chinese Academy of Sciences, Guangzhou 510640, China

† Electronic supplementary information (ESI) available: The SSW crystal pathway sampling method and the calculation details, the phase transition IS/FS pairs and the phase junction structures. See DOI: 10.1039/d1cp03415d

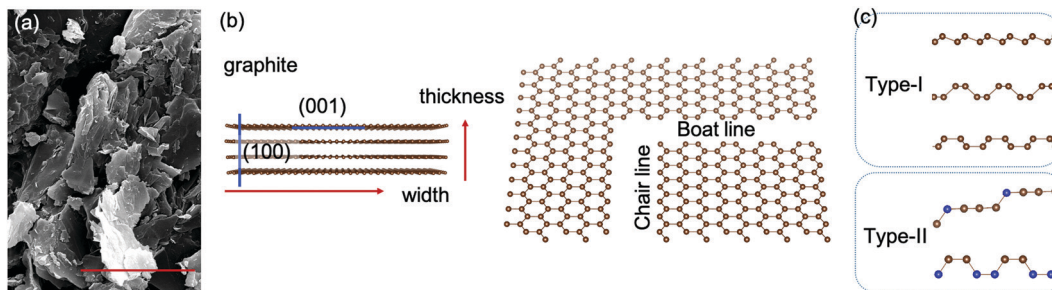


Fig. 1 (a) SEM image of the graphite grain (scale bar is 10 μm). (b) The atomic layers of graphite. (c) Two types of carbon layer: the twisting chair line and boat line.

Raman peaks of CD, Xu *et al.*¹⁵ reported that the high pressure carbon has a different bonding type from diamond for the absence of Raman peaks at the 1330 cm^{-1} range, which is the signature of CD and HD. By using synchrotron X-ray inelastic scattering and X-ray diffraction, Mao *et al.*⁶ found that both sp^2 and sp^3 bonding can co-exist in the high-pressure carbon allotrope with broadened XRD pattern. The high-pressure phase is superhard since it is an indented single crystal diamond. In short, the consensus is that the high-pressure carbon allotrope is a transparent and superhard material with co-existing sp^2/sp^3 bonding, only quenchable at low temperature (< 100 K), and the structure is different from that of CD or HD. However, to our best knowledge, our current experimental data are still insufficient to clarify the exact atomic structure.

On the theoretical side, researchers have devoted great efforts to predict the atomic structure of high-pressure carbon allotropes and the relative phase transition mechanisms. During the past decade, a lot of allotropic carbon structures have been proposed,^{16–19} such as layered diamond,²⁰ M-type carbon (monoclinic, $C2/m$, #12),^{21,22} W-type carbon (orthorhombic, $Pnma$, #62),²³ BCT structured carbon (tetragonal, $I4/mmm$, #139),²⁴ and Z-type (orthorhombic, $Cmmm$, #65) carbon.^{10,25} For example, by using the structure search method, Zhou *et al.*²⁶ predicted two families of carbon structures, both of which are packed by the regular bulking of five-type basic planes (in our opinion, three types of carbon layer, see Fig. 1c). *Via* a different bulking rule, Niu *et al.*²⁷ discovered three novel superhard carbon allotropes. However, contrary to experiments, those proposed structures are predicted to be mechanically stable at ambient conditions, and thus should be quenchable. The phase transition kinetics is critical to clarify the transition mechanism of room-temperature compressed carbon. Using the NEB method, Wang *et al.*²³ and Dong *et al.*²⁸ found that graphite-to-CD features the lowest energy barrier compared to other carbon allotropes when following the homogenous pathway, in which all atoms move within the unit cell. *Via* an advanced nucleation mechanism pathway, in which the transitions involve partial atom movements in the unit cell, Xiao *et al.*²⁹ and Xie *et al.*³⁰ found that graphite-to-HD is the most favorable among other competitive pathways. Those pioneering research studies point to the fact that the favorable transition pathways from graphite to the reported high-pressure carbon allotropes is still controversial. To date, neither the reported

structures nor the phase transition mechanism can fully explain the experimental observations.

Here, we use the stochastic surface walking method (SSW)^{30–32} integrated with the high-dimensional neural networks (HDNN) potential³³ to investigate the pathway mechanism of carbon allotropes. The candidate energy pathways obtained through the HDNN potential are further refined by DFT calculations to calculate the accurate energetics of the reaction. The DFT calculations were carried out by using the Vienna *ab initio* simulation package (VASP).³⁴ The exchange–correlation functional is parameterized by the local density approximation (LDA). By systematically exploring the low energy barrier pathways stemming from graphite, we show that the boat architecture line randomly shearing out of the graphite (001) basal plane contains the lowest energy barrier. This mechanism also predicts a variety of carbon allotropes with comparable free energies. The consequent shallow free energy welling leads to the co-existence of multiple carbon allotropes, thus resembling a topologically disordered structure. The disordering, as well as the predicted phase transition mechanism, have rationalized the previous experimental observation of the co-existing sp^2 and sp^3 bonding, amorphous-like broadened XRD peaks, the stiffened elastic properties, and the transition reversibility altogether.

The stochastic surface walking (SSW) method has successfully been used to predict the low-energy pathways of the crystal phase transitions, such as TiO_2 ³⁵ and FeO_2 ,³⁶ and will be the primary method to sample the free energy landscape of the carbon allotropes. Here, the pathway sampling was initially carried out in a unit cell of 8 carbon atoms. Through an exhaustive SSW sampling, thousands of initial/final state pairs were collected at 15 GPa. The transition state (TS) was located by the double-ended surface walking approach (DESW).³² Among the many reaction pairs, we found two disparate types of atomic movement that formulate the phase transition, namely, chair architecture line undulating and boat architecture line shearing. As reported by literature, most phase transitions are featured by undulating the chair architecture line layer-by-layer. This type of transition, named as the Type-I pathway, transforms the (001)_{GR} basal plane to an undulated sp^3 -hybridized carbon layer. Surprisingly, another major category of movement from our search belongs to the boat architecture line shearing type, named as the Type-II pathway. Instead of moving within the plane, this type of pathway has

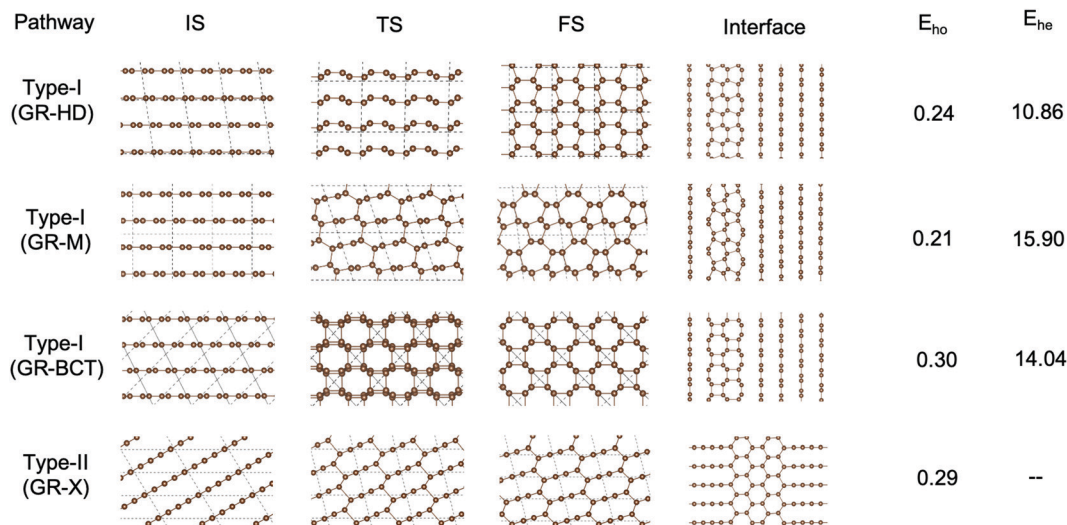


Fig. 2 The pathways of graphite to HD, BCT, M and X structure and the interface of the graphite and diamond, BCT, M and X structure. The structures in Type-I pathways are viewed down the $[100]_{\text{GR}}$ axis, while in the Type-II pathway, the structures are viewed down the $[120]_{\text{GR}}$ axis. The E_{ho} is in eV per atom and E_{he} is in eV.

bridging carbon atoms that can either shift up or down to form a sp^3 -hybridized carbon layer. As far as we know, the Type-II pathway has yet to draw much attention. Snapshots of the key structures of the two types of pathway are shown in Fig. 2.

For the Type-I pathway, the graphite (001) plane transits to the sp^3 -hybridized carbon layer *via* a layer-by-layer mechanism with propagation along the $[001]_{\text{GR}}$ direction. Fig. 2 lists the pathway from graphite to HD, BCT and M-structured carbon, respectively. For example, the graphite (001) plane transits to the boat architecture layer HD (100) with the orientation relation $(001)_{\text{GR}}// (100)_{\text{HD}}$, $[100]_{\text{GR}}// [010]_{\text{HD}}$. The energy barrier of graphite to HD is 0.24 eV per atom. In the pathway from graphite to the M carbon, the $(001)_{\text{GR}}$ basal plane transits to both zigzag architecture and chair architecture layer, and then bulks up to the M-type phase with the orientation relation $(001)_{\text{GR}}// (100)_{\text{M}}$, $[100]_{\text{GR}}// [010]_{\text{M}}$. The calculated energy barrier is 0.21 eV per atom. The BCT carbon phase is obtained by twisting the (001) basal plane to the boat architecture layer with the orientation relation $(001)_{\text{GR}}// (100)_{\text{BCT}}$, $[100]_{\text{GR}}// [001]_{\text{BCT}}$. The energy barrier of graphite to the BCT phase is 0.30 eV per atom. In those pathways, all of the carbon atoms in the unit cell transit to the sp^3 -bonded layer propagating along the $[001]_{\text{GR}}$ direction, namely, the homogenous pathway. While in the crystal nucleation, the $(001)_{\text{GR}}$ basal layer in the Type-I pathway turns into the undulating sp^3 architecture layers pathway, which naturally creates a coherent interface on the graphite $(001)_{\text{GR}}$ plane (Fig. 2). In this scenario, the formation of the nuclei core, as suggested by Xiao,²⁹ is required to proceed the phase transition. Here, we build a greater supercell of 128 carbon atoms that consists of a 3-layer nuclei core (the smallest core), to simulate the transition barrier. The nucleation energy barriers transiting to HD, M-type and BCT-carbon are 10.86, 15.90, and 14.04 eV, respectively. Our results support that the pathways from graphite to CD or HD have the lowest energy barrier among all three Type-I pathways. However, this is

against the experimental results, in which neither HD nor CD was observed.^{6,13,15}

The Type-II pathway is fundamentally different from Type-I. As shown in Fig. 2, the bridging atoms of the boat architecture line shears in the $[001]$ direction with the phase transition propagation along the graphite $[100]$ direction. Eying a typical movement along the pathway, the boat architecture line shifts out of the (001) basal plane to bond with the adjunction layer, forming a sp^3 bond, while the rest of the graphite carbons is stationary. The first step of this phase transition overcomes 0.29 eV per atom, which is higher than that of graphite to HD and graphite to M with the homogenous Type-I pathway. Interestingly, the metastable intermediate structure is a sp^3 -bonded layer, which is different from the Type-I pathway, where the smallest core needs three layers, indicating the high-pressure phase is formed without nuclei cores. Without a nuclei core, the overall kinetic barrier will be reduced substantially. Below, we set up a larger supercell to simulate this process and show how the Type-II pathway can proceed without forming nuclei cores.

Since the 8-atom unit cell is too small to embody the complexity of atom displacement, here, we enlarged the supercell up to 48-atom and recalculated possible pathways in the boat architecture line based on previous results (the surface phase transition energy profiles can be found in Fig. S1 in the ESI[†]). In the updated pool of IS/FS pairs, several newly discovered pathways belonging to the Type-II pathway were added. For clarity, we categorize two typical atomic movements that are the most energetically favored: pathways mainly involving single direction planar movements (namely Path-A), and pathways containing a mixture of upward and downward movements (namely Path-B). Fig. 3 summarizes the DFT energy profiles at 15 GPa and snapshots of typical movements along both types. On the left panel, carbon atoms shearing along one direction are depicted by the black arrow, signifying the

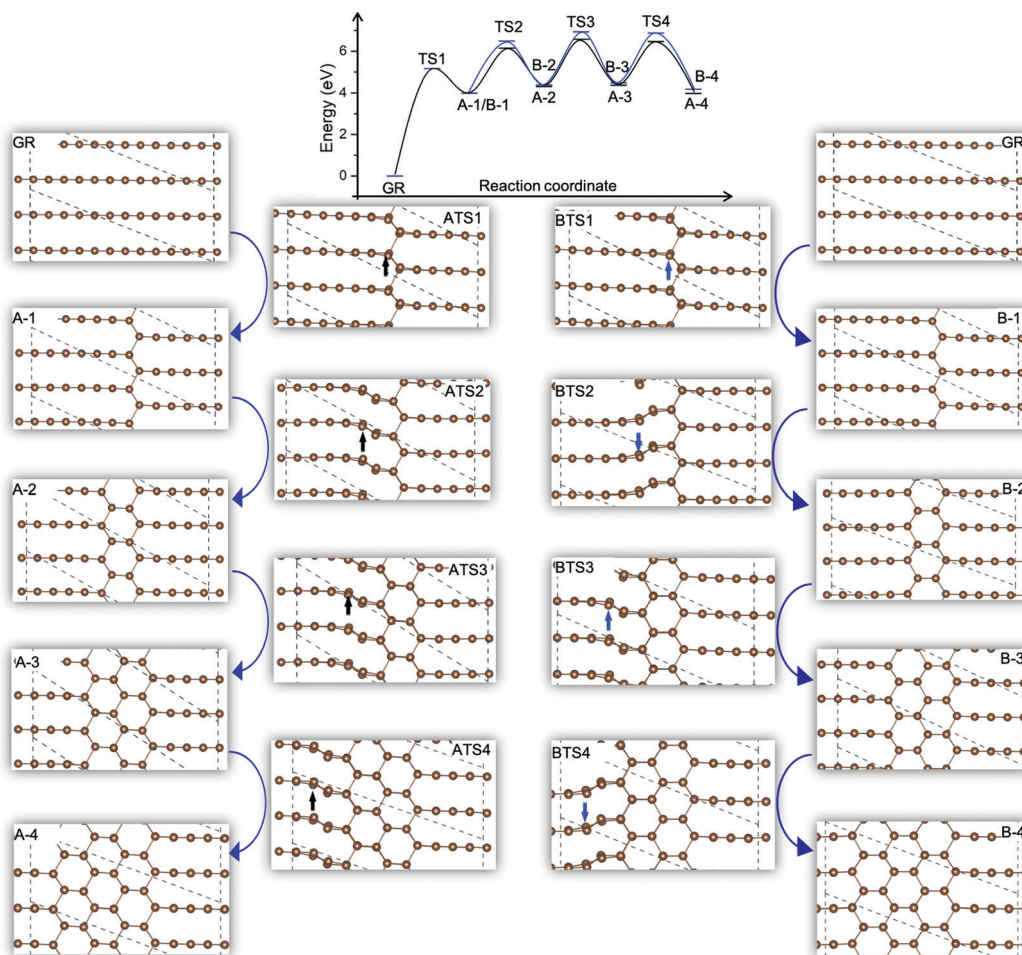


Fig. 3 Energy profiles and key structures initiating from graphite via step-by-step shearing. The left panel is Path-A, in which atoms shear along a single direction, the black line energy profiles; right panel is the Path-B in which atoms shear in two directions, the blue line energy profiles. Atomic movement and moving direction are depicted by arrows.

movement of Path-A. During the phase transition, the boat architecture line shears about $\sim 1/2S_d$ (S_d is the layer distance of the graphite (001) plane) to the middle of the graphite internal layer in the [001] direction. Simultaneously, the bridging carbons transform from sp^2 to sp^3 by bonding with carbon in the neighboring layer. That means the bridging carbons are obliged to shift horizontally, which breaks the six-fold symmetry of the graphite honeycomb sheet. Consequently, C_4 rings are formed when two carbon boat architecture lines are connected, while C_8 rings are surrounded by the C_4 ring. The sp^3 bonding in the C_4 ring features a 90° angle. On the other side, Path-B is a bi-direction shearing pathway. In the right panel of Fig. 3, the boat architecture line shears in two directions. Here, the C_4 rings are arranged in a zigzag line along the shearing direction. We summarize that both Path-A and Path-B require atomic movements only in one layer of carbon. Therefore, the kinetic barrier is expected to be lower than the previously acknowledged Type-I transition, which involves the movements from at least three layers of carbon atoms. The intermediate structure occupies the local minima position on the free energy landscape (Fig. 3, top inset), and are thus metastable

by definition. For this type of transition pathway, *via* a set of metastable structures, the transformation is similar to a stacking-fault-type phase transition.³⁷ However, with the proceeding of the phase transition, both enthalpy and the energy barrier increase slowly. This means that higher pressure is needed to drive the phase transition, which is consistent with Aust *et al.*⁴ and Montgomery *et al.*¹¹ that the phase transition takes place at 18 GPa, but the phase transition continues until approximately 60 GPa. The pressure-induced phase transitions mechanism also can be confirmed by the energy profiles in Fig. S1 in the ESI,[†] which are from a different pressure. We can find that the higher pressure will reduce the energy barrier both in Path-A and Path-B, as expected. For example, in the first step of Path-A, the energy barrier drops from 7.93 eV at 0 GPa, and 5.16 eV at 15 GPa to 3.90 eV at 30 GPa.

It should be emphasized that a great number of structures (see Fig. 4) could be constructed by changing the bridging spot and shearing direction *via* the Type-II pathway. For example, BCT carbon (tetragonal, $I4/mmm$, #139) is the product when the carbon sheet shears along one direction of boat architecture line, described by Path-A. Similarly, when the same carbon

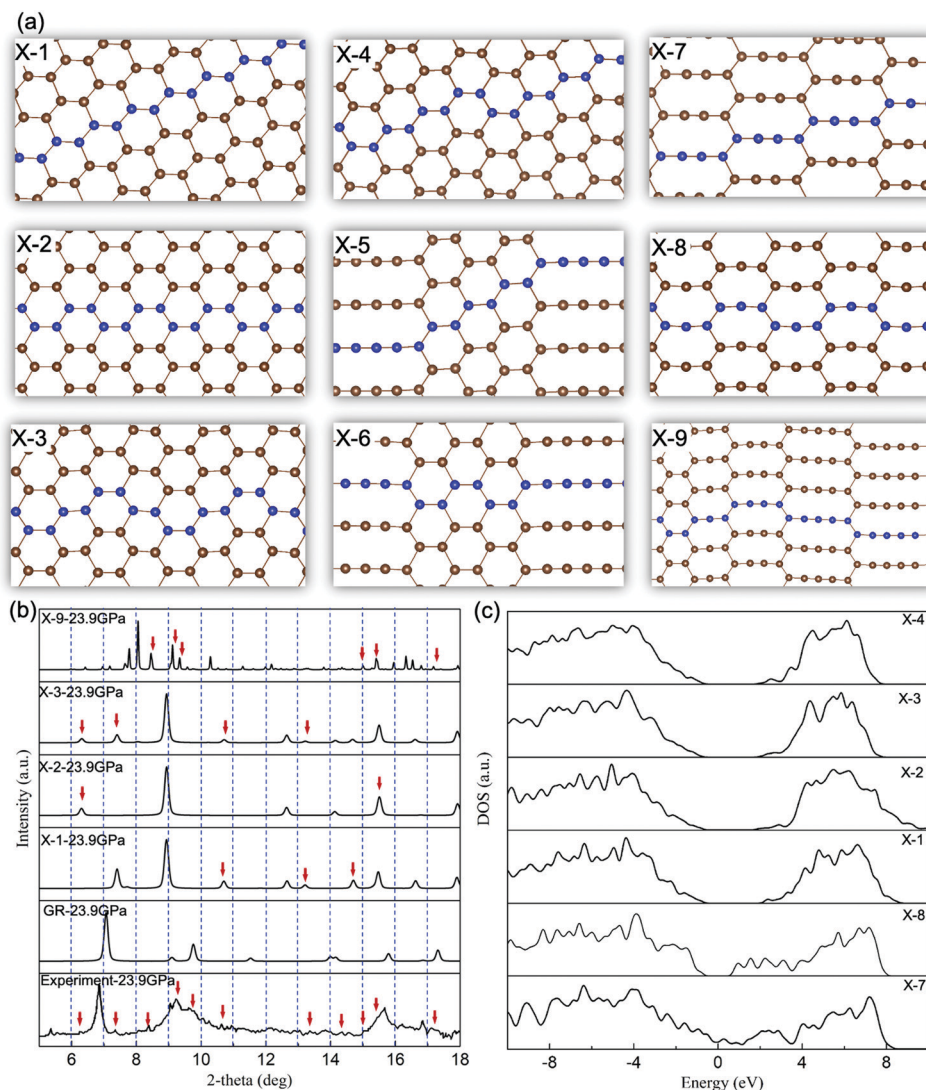


Fig. 4 (a) The structures formed by the Type-II mechanism, the blue line is from the same (001)_{GR} basal layer. (b) The simulation XRD results at 23.9 GPa and the experimental XRD results from ref. 6. (c) The density of state of carbon allotropes at 15 GPa.

sheet shears in both upward and downward directions, the final product will be an orthorhombic phase (*Cmca*, #64). On the other hand, the randomly separated sp^2 by sp^3 also adds plenty of structural complexity (shown as X5–X9 structures in Fig. 4). Mao *et al.*⁶ found that the transparency carbon is superhard since the high-pressure phase indented single crystals CD. Based on our calculation, the standard hardness of BCT carbon and the *Cmca* carbon are 91.4 and 90.2 GPa, respectively, which are comparable with CD (96.8 GPa) and HD (96.6 GPa). The structural variety according to the Type-II pathway may eventually lead to a disordering phase. In Fig. 4(b), we compared the simulation XRD results with those of the experimental XRD (ref. 6). The overlaid XRD patterns from simulation suggest that the broadened XRD along the 9–10 and 15–16 degrees in the experimental results can be explained by the assemblage of co-existing sp^2/sp^3 carbon. The coexistence of similar structures from the Type-II pathway can interpret the experimental observation of the broadened XRD patterns.

In the context of the experimental findings, our simulation results clarify the high-pressure carbon allotropes having coexisting sp^2 and sp^3 bonding. Both Raman spectra and inelastic scattering experiments suggested⁶ that both sp^2 and sp^3 bonding coexist in the same structure, rather than to be divided by grain boundaries.⁵ While previous first-principles simulation regarding high-pressure carbon allotropes are of either fully sp^3 or sp^2 bonding,^{10,21–25} the coexisting sp^2 and sp^3 are more likely to exist in separated domains due to thermodynamic hysteresis. Therefore, the high-pressure phase was referred to the mixing of a full sp^3 structure and sp^2 graphite in macro, separated by crystal grain boundaries, which is contrary to experimental observation. Therefore, due to its lower kinetic barrier, the Type-II pathway is a more preferred transition mechanism for room-temperature compressed carbon. During the transition, the sp^2 and sp^3 carbons are bonded together in the atomic level. The unreacted graphite is sliced into fragments by random sp^3 bridging carbons. The mixed sp^2/sp^3

bonding also explains the puzzle about the electrical conductivity under pressure. The suddenly increased resistivity above 18 GPa may be due to the sp^3 carbon reaching a shield percentage. Since the sp^2 and sp^3 bonding are mixed in the atomic level, according to the percolation theory,³⁸ the product phase becomes transparent when the sp^3 -carbon reaches a shield percentage.

The second issue is the reversibility of the phase transition in carbon.⁵ The conventional Type-I pathway requires the existence of the nuclei core, which allows for the separated sp^2 phase and sp^3 phase in two grains domains. However, as we know, both nanocrystalline sp^3 -carbon and nanocrystalline graphite are kinetically stable under ambient condition.³⁹ Thus, as Miller⁵ suggested, the high pressure carbon phase should be organized differently from mixtures of these phases in macro. Our results suggest that the sp^2 and sp^3 carbons are bonded together at the atomic level in the X-phase. Under high pressure, the metastable nature of the single sp^3 -carbon layer, built up during the phase transition, leads to a favorable transition pathway without the prerequisite of forming the nuclei core. While under decompression, the sp^3 -hybridized bonds in the single sp^3 -carbon layer become unstable, suggesting the transition is reversible after removing pressure.

Finally, we are at the position to discuss the anisotropic kinetics of graphite under pressure. Since the thickness of the (001)_{GR} plane is of a magnitude-level greater than that of the (100)_{GR} plane (Fig. 1), this implies that graphite was preferred to be orientated along the [001]_{GR} direction in the diamond anvil cell under pressure. In such case, the phase transition pathway is sensitive to the local strain and the crystallographic orientation. The deviatoric force is more easily applied along the [001]_{GR} direction than [100]_{GR}, which will induce the shearing movement. Miller's experiment⁵ noticed that the center of compressed graphite is more transparent than its surrounding areas, which can be regarded as the results of anisotropy. Despite being thermodynamically less stable, high-pressure carbon allotropes from the Type-II pathway are chosen by phase transition kinetics because of its lower energy barrier.

In summary, our work attempts to resolve the atomistic structure and relative phase transition mechanism of graphite under room temperature compression. By shearing the boat architecture line atoms out of the graphite (001) plane upward or downward, the bridging carbon atoms transit to sp^3 -hybrid bonding, forming the C_4 ring. Since the carbon atoms shear in different directions and the randomly bridging spot, the mechanism yields a variety of carbon allotropes with similar free energies, possessing a broadened XRD pattern. We suggest that shearing the boat architecture line in the [001] direction is kinetically preferred because there is no need to form the nuclei core. *Vice versa*, the (meta-)stable nature of the intermediate state ensures that the phase transition is reversible upon decompression. The proposed structures and phase transition mechanism rationalize the issues of the broadened XRD, the superhard properties, the suddenly increasing electrical resistivity, the co-existing sp^2 and sp^3 , and the reversible phase transition. Understanding this mechanism may help better design superhard carbon materials.

Author contributions

Sheng-cai Zhu conceived the research idea, performed the calculations and analyzed the simulation data. Sheng-cai Zhu and Qing-yang Hu wrote and revised the manuscript.

Conflicts of interest

The authors declare no competing financial interests.

Acknowledgements

S. C. Z. is supported by the National Science Foundation of China (Grant No. 21703004) and the Hundreds of Talents Program of Sun Yat-sen University. Q. Y. H. is supported by the CAEP Research Project (CX20210048) and a Tencent Xplore prize. We thank Zhi-Pan Liu for helping to construct the NN potential. We also acknowledge the use of computing resources from the Tianhe-2 Supercomputer.

References

- 1 H. Shin, S. Kang, J. Koo, H. Lee, J. Kim and Y. Kwon, Cohesion Energetics of Carbon Allotropes: quantum Monte Carlo Study, *J. Chem. Phys.*, 2014, **140**, 11.
- 2 D. Selli, I. A. Baburin, R. Martoňák and S. Leoni, Superhard Sp^3 Carbon Allotropes with Odd and Even Ring Topologies, *Phys. Rev. B: Condens. Matter Mater. Phys.*, 2011, **84**(16), 161411.
- 3 S. Zhu, X. Yan, J. Liu, A. R. Oganov and Q. Zhu, A Revisited Mechanism of the Graphite-to-Diamond Transition at High Temperature, *Matter*, 2020, **3**(3), 864–878.
- 4 R. B. Aust and H. G. Drickamer, Carbon: a New Crystalline Phase, *Science*, 1963, **140**(3568), 817–819.
- 5 E. D. Miller, D. C. Nesting and J. V. Badding, Quenched Transparent Phase of Carbon, *Chem. Mater.*, 1997, **9**(1), 18–22.
- 6 W. L. Mao, Bonding Changes in Compressed Superhard Graphite, *Science*, 2003, **302**(5644), 425–427.
- 7 M. Hanfland, K. Syassen and R. Sonnenschein, Optical Reflectivity of Graphite under Pressure, *Phys. Rev. B: Condens. Matter Mater. Phys.*, 1989, **40**(3), 1951–1954.
- 8 Y. X. Zhao and I. L. Spain, X-Ray Diffraction Data for Graphite to 20 GPa, *Phys. Rev. B: Condens. Matter Mater. Phys.*, 1989, **40**(2), 993–997.
- 9 F. P. Bundy and J. S. Kasper, Hexagonal Diamond – A New Form of Carbon, *J. Chem. Phys.*, 1967, **46**(9), 3437–3446.
- 10 Y. Wang, J. E. Panzik, B. Kiefer and K. K. M. Lee, Crystal Structure of Graphite under Room-Temperature Compression and Decompression, *Sci. Rep.*, 2012, **2**(1), 520.
- 11 J. M. Montgomery, B. Kiefer and K. K. M. Lee, Determining the High-Pressure Phase Transition in Highly-Ordered Pyrolytic Graphite with Time-Dependent Electrical Resistance Measurements, *J. Appl. Phys.*, 2011, **110**(4), 043725.
- 12 T. Yagi, W. Utsumi, M. Yamakata, T. Kikegawa and O. Shimomura, High-Pressure *In Situ* X-ray-Diffraction Study

- of the Phase Transformation from Graphite to Hexagonal Diamond at Room Temperature, *Phys. Rev. B: Condens. Matter Mater. Phys.*, 1992, **46**(10), 6031–6039.
- 13 W. Utsumi and T. Yagi, Light-Transparent Phase Formed by Room-Temperature Compression of Graphite, *Science*, 1991, **252**(5012), 1542–1544.
 - 14 M. Hanfland, H. Beister and K. Syassen, Graphite under Pressure: equation of State and First-Order Raman Modes, *Phys. Rev. B: Condens. Matter Mater. Phys.*, 1989, **39**(17), 12598–12603.
 - 15 J. A. Xu, H. K. Mao and R. J. Hemley, The Gem Anvil Cell: high-Pressure Behaviour of Diamond and Related Materials, *J. Phys.: Condens. Matter*, 2002, **14**(44), 11549–11552.
 - 16 D. Selli, I. A. Baburin, R. Martoňák and S. Leoni, Superhard Sp^3 Carbon Allotropes with Odd and Even Ring Topologies, *Phys. Rev. B: Condens. Matter Mater. Phys.*, 2011, **84**(16), 161411.
 - 17 X.-F. Zhou, G.-R. Qian, X. Dong, L. Zhang, Y. Tian and H.-T. Wang, *Ab initio* Study of the Formation of Transparent Carbon under Pressure, *Phys. Rev. B: Condens. Matter Mater. Phys.*, 2010, **82**(13), 134126.
 - 18 C. He, L. Sun, C. Zhang, X. Peng, K. Zhang and J. Zhong, New Superhard Carbon Phases between Graphite and Diamond, *Solid State Commun.*, 2012, **152**(16), 1560–1563.
 - 19 M. J. Xing, B. H. Li, Z. T. Yu and Q. Chen, Monoclinic $C2/m-20$ Carbon: a Novel Superhard Sp^3 Carbon Allotrope, *RSC Adv.*, 2016, **6**(39), 32740–32745.
 - 20 F. J. Ribeiro, P. Tangney, S. G. Louie and M. L. Cohen, Structural and Electronic Properties of Carbon in Hybrid Diamond-Graphite Structures, *Phys. Rev. B: Condens. Matter Mater. Phys.*, 2005, **72**(21), 214109.
 - 21 Q. Li, Y. Ma, A. R. Oganov, H. Wang, H. Wang, Y. Xu, T. Cui, H. Mao and G. Zou, Superhard Monoclinic Polymorph of Carbon, *Phys. Rev. Lett.*, 2009, **102**(17), 175506.
 - 22 A. R. Oganov and C. W. Glass, Crystal Structure Prediction Using *Ab Initio* Evolutionary Techniques: principles and Applications, *J. Chem. Phys.*, 2006, **124**(24), 244704.
 - 23 J.-T. Wang, C. Chen and Y. Kawazoe, Low-Temperature Phase Transformation from Graphite to Sp^3 Orthorhombic Carbon, *Phys. Rev. Lett.*, 2011, **106**(7), 075501.
 - 24 K. Umemoto, R. M. Wentzcovitch, S. Saito and T. Miyake, Body-Centered Tetragonal C4: a Viable Sp^3 Carbon Allotrope, *Phys. Rev. Lett.*, 2010, **104**(12), 125504.
 - 25 Z. Zhao, B. Xu, X. F. Zhou, L. M. Wang, B. Wen, J. He, Z. Liu, H. T. Wang and Y. Tian, Novel Superhard Carbon: C-Centered Orthorhombic C8, *Phys. Rev. Lett.*, 2011, **107**(21), 1–5.
 - 26 R. Zhou and X. C. Zeng, Polymorphic Phases of Sp^3 -Hybridized Carbon under Cold Compression, *J. Am. Chem. Soc.*, 2012, **134**(17), 7530–7538.
 - 27 H. Niu, X.-Q. Chen, S. Wang, D. Li, W. L. Mao and Y. Li, Families of Superhard Crystalline Carbon Allotropes Constructed *via* Cold Compression of Graphite and Nanotubes, *Phys. Rev. Lett.*, 2012, **108**(13), 135501.
 - 28 X. Dong, X.-F. Zhou, G.-R. Qian, Z. Zhao, Y. Tian and H.-T. Wang, An *Ab Initio* Study on the Transition Paths from Graphite to Diamond under Pressure, *J. Phys.: Condens. Matter*, 2013, **25**(14), 145402.
 - 29 P. Xiao and G. Henkelman, Communication: from Graphite to Diamond: reaction Pathways of the Phase Transition, *J. Chem. Phys.*, 2012, **137**, 10.
 - 30 C. Shang and Z.-P. Liu, Stochastic Surface Walking Method for Structure Prediction and Pathway Searching, *J. Chem. Theory Comput.*, 2013, **9**(3), 1838–1845.
 - 31 C. Shang, X.-J. Zhang and Z.-P. Liu, Stochastic Surface Walking Method for Crystal Structure and Phase Transition Pathway Prediction, *Phys. Chem. Chem. Phys.*, 2014, **16**(33), 17845–17856.
 - 32 X.-J. Zhang and Z.-P. Liu, Variable-Cell Double-Ended Surface Walking Method for Fast Transition State Location of Solid Phase Transitions, *J. Chem. Theory Comput.*, 2015, **11**(10), 4885–4894.
 - 33 S.-D. Huang, C. Shang, X.-J. Zhang and Z.-P. Liu, Material Discovery by Combining Stochastic Surface Walking Global Optimization with a Neural Network, *Chem. Sci.*, 2017, **8**(9), 6327–6337.
 - 34 G. Kresse and J. Furthmüller, Efficient Iterative Schemes for *Ab Initio* Total-Energy Calculations Using a Plane-Wave Basis Set, *Phys. Rev. B: Condens. Matter Mater. Phys.*, 1996, **54**(16), 11169.
 - 35 S.-C. Zhu, S.-H. Xie and Z.-P. Liu, Nature of Rutile Nuclei in Anatase-to-Rutile Phase Transition, *J. Am. Chem. Soc.*, 2015, **137**(35), 11532–11539.
 - 36 S. Zhu, Q. Hu, W. L. Mao, H. Mao and H. Sheng, Hydrogen-Bond Symmetrization Breakdown and Dehydrogenation Mechanism of FeO_2H at High Pressure, *J. Am. Chem. Soc.*, 2017, **139**(35), 12129–12132.
 - 37 A. R. Oganov, R. Martoňák, A. Laio, P. Raiteri and M. Parrinello, Anisotropy of Earth's D'' Layer and Stacking Faults in the MgSiO_3 Post-Perovskite Phase, *Nature*, 2005, **438**(7071), 1142–1144.
 - 38 A. A. Saberi, Recent Advances in Percolation Theory and Its Applications, *Phys. Rep.*, 2015, **578**, 1–32.
 - 39 X. Ma, X. Liu, Y. Li, X. Xi, Q. Yao and J. Fan, Influence of Crystallization Temperature on Fluorescence of *n*-Diamond Quantum Dots, *Nanotechnology*, 2020, **31**(50), 505712.